npj | precision oncology

Article

Published in partnership with The Hormel Institute, University of Minnesota

https://doi.org/10.1038/s41698-024-00777-6

Genomic scarring score predicts the response to PARP inhibitors in non-small cell lung cancer

Katerina Tsilingiri[1,9], Anna Chalari[1,9], Georgia Christopoulou[2], Alexandra Voutsina[3], Pantelis Constantoulakis[2], Konstantinos Potaris[4], Ioannis Vamvakaris[5], Dora Hatzidaki[6], Georgina Zachou[6], Giannis Vatsellas[7], Vassilis Georgoulias[6], Athanasios Kotsakis[8] & Apostolos Klinakis[1] ✉

PARP inhibitors (PARPi) have shown efficacy in tumours harbouring mutations in homologous recombination repair (HRR) genes. Somatic HRR mutations have been described in patients with Non-Small Cell Lung Cancer (NSCLC), but PARP inhibitors (PARPi) are not yet a therapeutic option. Here we assessed the homologous recombination status of early-stage NSCLC and explored the therapeutic benefit of PARPi in preclinical models. The Genomic Scarring Score GSS (GSS) and HRR mutation profile of 136 patients were assessed. High GSS (h-GSS) was observed in 39 (28.7%) patients half of which carried pathogenic/likely pathogenic somatic HRR mutations. TP53 mutations were significantly enriched in h-GSS tumours ($p < 0.001$). Olaparib significantly delayed tumour growth in h-GSS but not l-GSS Patient-derived Xenografts (PDXs), while patients with h-GSS/TP53mut tumours respond favourably to adjuvant platinum-based chemotherapy. Our functional data clearly support the idea that the use of GSS rather than the mutational status of HRR genes could select patients for administration of PARPi.

Double strand breaks (DSBs) are considered the most dangerous DNA lesions in proliferating cells. Different mechanisms with variable fidelity mediate DSB repair. Homologous recombination (HR), occurring exclusively in cells that have duplicated their DNA, is the non-error-prone mechanism of DSB repair. *BRCA1* and *BRCA2* genes encode critical components of the HR repair machinery, while inactivating mutations or allelic loss lead to HR deficiency (HRD)[1]. Cells lacking *BRCA1/2* activity are sensitive to poly(ADP-ribose) polymerase (PARP1/2) inhibition[2,3]. These findings exposed a therapeutic vulnerability and led to the development of PARP1/2 inhibitors (PARPi) which trap the PARP proteins in the DNA by forming PARP-DNA complexes. These complexes act as physical blocks in DSB repair, leading to replication fork stalling and collapse, and eventually unrepaired lesions and cell death.

Since the original demonstration that women with germline mutations in *BRCA1* and *BRCA2* are at risk of developing ovarian and breast cancer, the FDA approved the therapeutic use of PARPi for patients with breast and ovarian cancer and, more recently, in patients with prostate and pancreatic cancer harbouring *BRCA1/BRCA2* gene mutations[4–7]. In addition to *BRCA1* and *BRCA2* loss, HRD can be the result of mutation or biallelic loss of other HR components across tumour types[8]. The complexity of HRD genetics has led to the development of surrogate markers for HRD, either functionally monitoring the activity of the HR machinery through quantitation of the HR marker RAD51[9] or by assessing the result of HRD in the genome through next-generation sequencing. In fact, next-generation sequencing assessing loss of heterozygosity (LOH), telomeric-allelic imbalance (TAI) and large-scale state transitions (LST) leads to measurable indicators of genomic instability, the genomic scarring score (GSS), which can be used to assess HRD. A published meta-analysis of existing data from 8847 cases across 33 cancer types (including non-small cell lung cancer-NSCLC) revealed

[1]Biomedical Research Foundation of the Academy of Athens, Athens, Greece. [2]Genotypos MSA, Private Molecular Biology and Cytogenetics Diagnostic Center, Athens, Greece. [3]Institute of Chemical Biology, National Hellenic Research Foundation, Athens, Greece. [4]Department of Thoracic Surgery, "SOTIRIA" General Hospital, Athens, Greece. [5]Department of Pathology, "SOTIRIA" General Hospital, Athens, Greece. [6]Hellenic Oncology Research Group, Athens, Greece. [7]Greek Genome Centre, Biomedical Research Foundation of the Academy of Athens, Athens, Greece. [8]Department of Medical Oncology, University General Hospital of Larisa, Larisa, Greece. [9]These authors contributed equally: Katerina Tsilingiri, Anna Chalari. ✉e-mail: aklinakis@bioacademy.gr

THE HORMEL INSTITUTE
UNIVERSITY OF MINNESOTA

that 18% had a positive HRD score (GSS > 42)[10], but of those, only 4% carried deleterious mutations in either *BRCA1* or *BRCA2* and only 26% carried deleterious mutations in other HRR genes[11]. In the same study, positive HRD scores were detected in 51% of primary lung squamous cell carcinoma (LUSC) and 35.8% of primary lung adenocarcinoma (LUAD) but again, only in about 40% of the tumours could this high GSS be attributed to deleterious HRR gene mutations. Other studies have indicated high GSS (h-GSS) scores ranging from 18.7% to 66% for advanced NSCLC[12,13], whereas another study reports an association of high GSS and loss-of-function mutations in several tumour suppressor genes, including TP53, LRP1B and CDKN2A, supporting the notion that HRD could be driven by non-HRR gene mutations. Conversely, mutations in oncogenes were more prevalent in the low GSS subpopulation[14].

A recently published randomized placebo-controlled phase II study of maintenance of the PARPi olaparib in stage IV NSCLC patients, who achieved disease control with front-line platinum-based chemotherapy (PIN trial), demonstrated a numerically greater but not statistically significant PFS in favour of the olaparib group; although patient enrolment was based only on their clinical responsiveness to platinum-based chemotherapy, a subgroup analysis revealed a significant benefit in smoker patients treated with olaparib suggesting that this should be attributed to HRD-related genetic alterations[15].

In the current study, we sought to assess the HRD status of early-stage NSCLC tumours based on the GSS score. The use of surgical material, only available for early-stage operable NSCLC, allows the establishment of patient-derived xenografts (PDXs), which we have used as a model to functionally investigate the efficacy of PARPi. PDX with h-GSS showed a lower RAD51 foci count upon damage induction and a favourable response to olaparib independently of the presence of HRR gene alterations, indicating that GSS can be used as a predictive biomarker for PARPi response to better stratify NSCLC patients for treatment with PARPi.

Results

Genomic scarring score and HRR gene mutations

Thirty-nine (28.7%) patients were found to have a high GSS (50 and higher, h-GSS) and 97 a low score (ranging from 0 to 49; l-GSS) (Fig. 1A). Among patients with h-GSS and l-GSS, 30 (76.9%) had a score >70 and 66 (68%) a score <10, respectively ($p < 0.001$; Fig. 1B). There was no correlation between the histologic subtypes, the disease stage and the smoking status and the high or low GSS. HRR variants (both P/LP and VUS) were identified in 18/39 (46.2%) of h-GSS and in 37/97 (38.1%) of l-GSS primary tumours, ($p = 0.389$). Thirteen (33.3%) patients with h-GSS and 18 (18.6%) with l-GSS carried pathogenic or likely pathogenic (P/LP) HRR variants showing an enrichment of P/LP mutations in the h-GSS group ($p = 0.063$).

Among the P/LP HRR mutations, 3 (7.7%) in the h-GSS and 2 (2.1%) in the l-GSS subgroup were germline variants. Somatic mutation analysis revealed that only 13/39 (33.3%) of the observed h-GSS tumours could be attributed to P/LP mutations in HRR genes (Fig. 1C). At the same time, P/LP mutations in HRR genes were present in 18/97 (18.6%) patients with l-GSS (Fig. 1C). Finally, HRR gene mutations characterized as variants of unknown significance (VUS) were identified in 12.8% ($n = 5$) and 19.6% ($n = 19$) with h-GSS and l-GSS, respectively (Fig. 1C).

HRR gene expression and RAD51 foci formation in primary tumours

Since HRR gene mutation status alone cannot explain the high GSS score, we reasoned that h-GSS tumours might present a down-regulation of the HRR gene expression. However, mRNA expression levels of HRR genes did not show significant differences between low and high GSS tumours, (Fig. 2A and Supplementary Table 1). Nevertheless, as RAD51C expression was unexpectedly higher in h-GSS tumours, we compared the formation of RAD51 foci between h-GSS and l-GSS tumours. As expected, h-GSS tumours presented almost no foci, strongly indicating a failure to assemble a functional HRR complex. (Fig. 2B and Supplementary Table 2).

GSS and p53 status

Previous studies have shown an association between the GSS and the mutation status of *TP53* in different tumour types[11,16]. We thus investigated the presence and the variant allele frequency of the TP53 mutations in h-GSS and l-GSS tumours. The prevalence of pathogenic

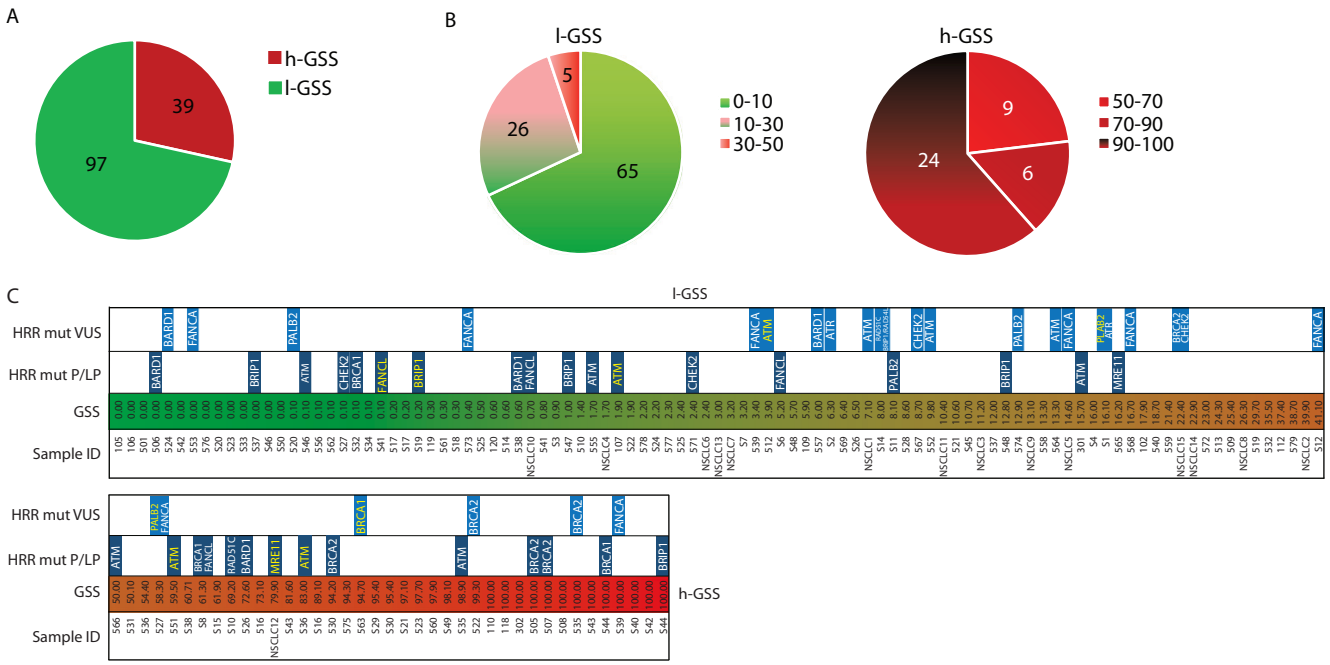

Fig. 1 | GSS and HR gene mutations in an early NSCLC patient cohort. A Number of l-GSS and h-GSS tumours in the patient cohort. **B** Break-down of the different subgroups of l-GSS and h-GSS tumours across the GSS scale. **C** Heat map of HRR-related P/LP and VUS mutations. Germline mutations are shown in yellow font. In cases with P/LP mutations, VUS are not shown.

p53 mutations was higher in h-GSS than in l-GSS primary tumours (94.9% vs 51.5%, $p < 0.001$; Fig. 3A, B, Table 1). Additionally, 50 (51.5%) of the patients with l-GSS tumours carried pathogenic *TP53* mutations and 27 of these tumours had a GSS < 10 (Table 2). Variant Allele Frequency (VAF) of the TP53 mutations showed a significant correlation with GSS (Fig. 3C; $r = 0.5648$, $p < 0.0001$). No association was observed between the VAF of HRR mutations and GSS or between the VAF of TP53 mutations and HRR gene mutations

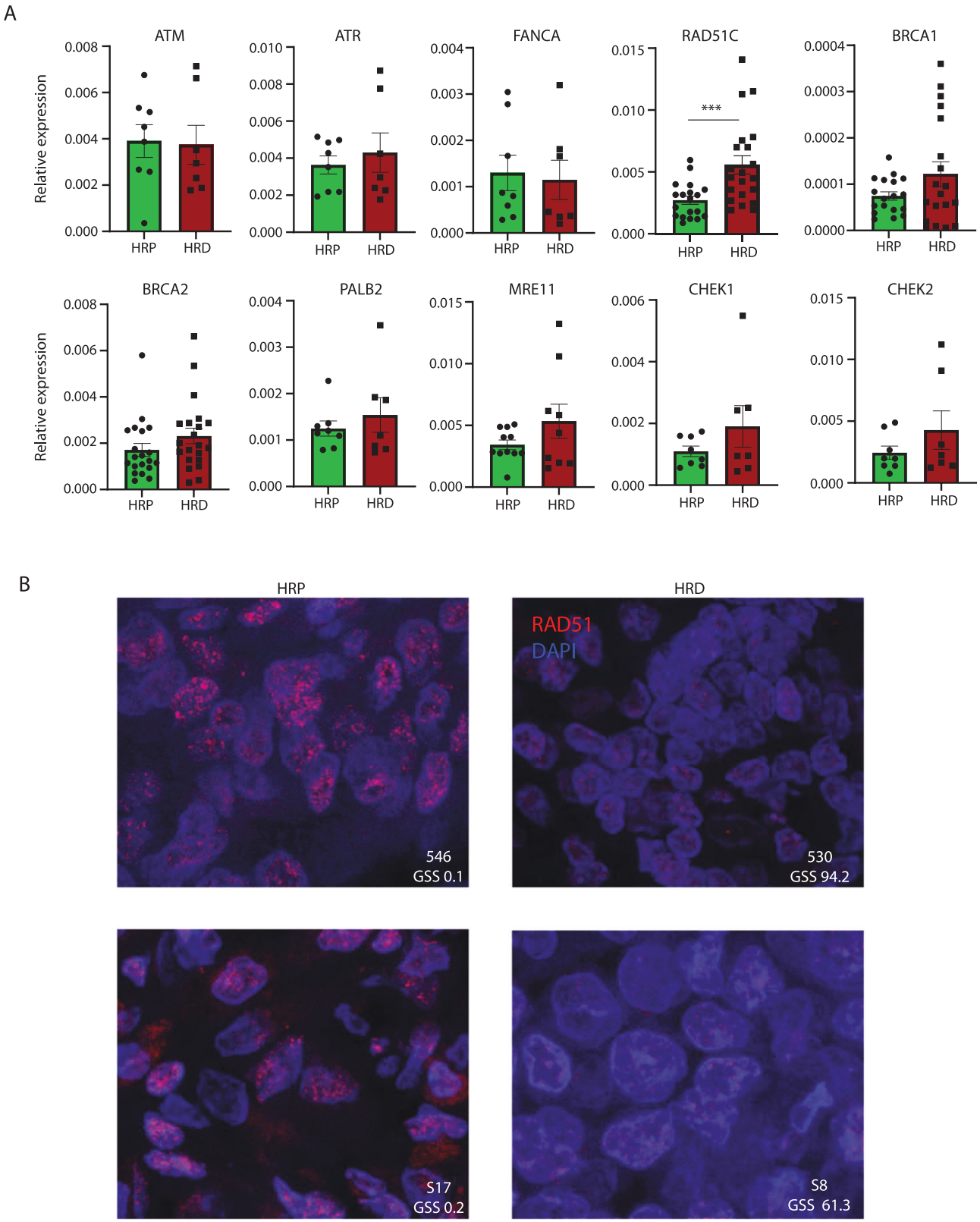

Fig. 2 | HR gene expression and RAD51 status in the NSCLC cohort. A mRNA expression of HR genes in l-GSS (left) vs h-GSS (right) tumours, expression is normalized against β-actin, ***: $p < 0.001$, n = at least 8 samples/group. **B** RAD51 foci formation in l-GSS vs h-GSS primary tumours, pictures are representative from $n = 8$ patients/group.

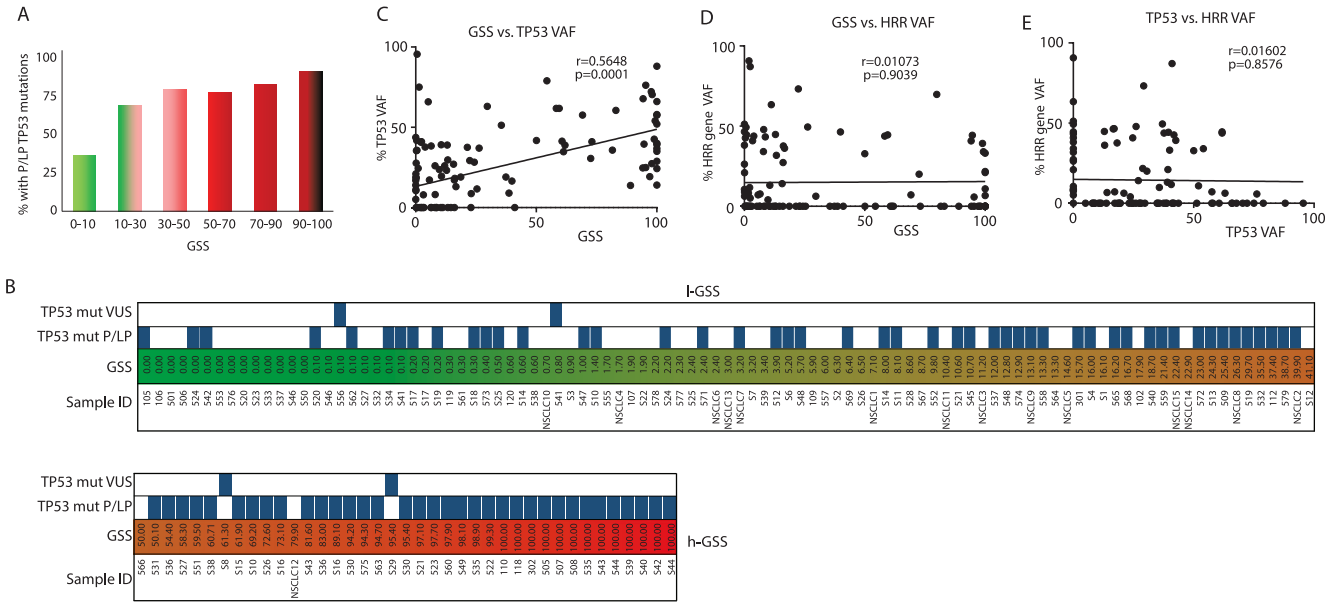

Fig. 3 | Correlation of TP53 status with GSS. A Prevalence of P/LP TP53 mutations across the GSS scale. **B** Heat map of TP53 P/LP and VUS mutations. **C** Correlation of GSS score and TP53 mutation VAF. **D** Correlation of GSS score and HRR VAF. **E** Correlation of TP53 and HRR VAF. For samples with more than one HRR mutation, the sum of VAFs of the separate mutations is plotted. In cases with P/LP mutations, VUS are not shown.

Table 1 | Presence or absence of TP53 mutations in each of the two GSS groups (All pts)

All pts (*N* = 136)	GSS score		
	l-GSS (*n* = 97)	h-GSS (*n* = 39)	*p*-value
TP53 yes (*n* = 87)	50 (51.5%)	37 (94.9%)	**<0.001** (Fisher's)
TP53 no (n = 49)	47 (48.5%)	2 (5.1%)	

(P/LP or VUS) in either h-GSS or l-GSS tumours (Fig. 3D, E and Supplementary Table 2).

Effect of CDDP and olaparib in h-GSS and l-GSS tumours

The engraftment success rate was approximately 60%, matching previous reports of our lab and others[17–19]. To ascertain that PDX models recapitulate the RAD51 pattern of the primary tumour, we compared the frequency of RAD51 foci in formalin-fixed paraffin-embedded (FFPE) samples of the primary tumour and respective PDXs (molecular profiles and GSS in Supplementary Table 2). As Fig. 4A indicates, primary tumours and PDXs present similar RAD51 foci frequencies under steady-state conditions, which are generally low irrespective of the GSS. This probably reflects the low damage levels in the absence of DNA-damaging agents. Whether this is a peculiarity of early-stage NSCLC is still under investigation (baseline RAD51 scores of PDXs can be found in Supplementary Table 3).

Expression of RAD51 in steady-state was detectable in both l-GSS and h-GSS PDXs, although the number of foci/nucleus was low and not significantly different between the two groups (Fig. 4B). However, in CDDP-treated l-GSS PDX, the number of nuclei with >10 RAD51 foci drastically increased compared to the untreated PDX, whereas this was not the case in h-GSS PDX, which had a significantly lower ($p = 0.016$) number of foci-rich nuclei (Fig. 4C). To evaluate whether PARP inhibition would be efficient in HRD NSCLC, we compared the efficacy of olaparib on h-GSS and l-GSS PDXs. h-GSS PDXs showed a significant, albeit partial response to olaparib, as tumour growth was significantly slower compared to the untreated group; conversely, l-GSS PDXs did not respond to olaparib treatment and grew similarly to untreated PDXs (Fig. 5).

Clinical outcome according to GSS and TP53 status

After a median follow-up period of 47.9 months (range: 0.1-68.6 mo), there were 45 (33.1%) recurrences and 30 (22.1%) deaths due to disease progression (Table 3). The 2- and 3-year survival rates were 85% and 75.7%, respectively. Seventy-two (52.9%) patients received adjuvant platinum-based chemotherapy and 7 (5.1%) had adjuvant radiotherapy. The median DFI and OS have not been reached (range 0.1–68.4 mo), and there was no significant difference between l-GSS and h-GSS patients, both in the whole cohort of patients as well as in the subgroup of patients who received platinum-based adjuvant chemotherapy (DFI: $p = 0.82$; OS: $p = 0.23$). Nevertheless, after univariate analysis, the co-existence of h-GSS and TP53 mutations (h-GSS/TP53mut subgroup of patients: $n = 27$) was associated with a significantly higher DFI compared to patients with l-GSS/TP53 wt [$n = 17$; 35.9 mo vs 21.7 mo, ($p = 0.012$)]; [Fig. 6A and Supplementary Table 4a], while no other covariate reached statistical significance, alone or in conjunction with GSS/TP53 status (not shown). Moreover, patients with h-GSS/TP53mut tumours who received platinum-based chemotherapy at any setting (adjuvant and/or metastatic) had significantly better OS (non-reached vs. 28.5 mo; $p = 0.004$; Fig. 6B and Supplementary Table 4b).

Discussion

Exploiting DNA repair in cancer therapeutics has become a field of extensive research in recent years[20], with the repair of DSBs being at the forefront of this research due to the defects of the HR repair machinery. HRD is present in various tumour types and is traditionally associated with germline or somatic mutations in *BRCA1/BRCA2* or other genes of the HRR machinery[21,22]. The discovery of PARP inhibitors and the concept of synthetic lethality has been a major breakthrough in the treatment of tumours such as breast and ovarian cancer as well as prostate and pancreatic adenocarcinoma, in which germ-line and somatic mutations in the *BRCA1/2* genes are relatively common. However, patients with mutated BRCA1/2 do not always respond to PARP inhibition[23], while on the other hand, patients who do not harbour BRCA1/2 or other HRR-related gene mutations inexplicably do respond[24]. Thus, it appears that homologous recombination deficiency can be a result of yet unidentified mechanisms, highlighting the need for novel stratification methods to determine which patients might benefit from PARPi administration.

Table 2 | TP53 and GSS score (All pts)

All pts (*N* = 136)	GSS score			
	<10 (*n* = 66)	≥10–≤70 (*n* = 40)	>70 (*n* = 30)	*p*-value
TP53 yes (*n* = 87)	27 (40.9%)	31 (77.5%)	29 (96.7%)	**<0.001** (Fisher's)
TP53 no (*n* = 49)	39 (59.1%)	9 (22.5%)	1 (3.3%)	

Next-generation sequencing allowed the identification of genomic scarring signatures initially associated with germ-line *BRCA1/2* mutations. However, these were subsequently identified in a wide spectrum of solid malignancies and independently of *BRCA1/2* mutation status[25,26]. Several clinically approved, commercially available or academic algorithm platforms have been developed to predict HRD based on DNA (whole genome or whole exome sequencing) or gene expression (RNA sequencing) data[27,28], and they have provided an excellent opportunity to expand the patient groups which could benefit from PARPi in the clinic. These platforms examine the presence of certain 'genomic scars' which arise when the cell fails to properly carry out the homologous recombination repair. Based on the presence of such scars, the predictive algorithms assign a 'score' between 0 and 100. Then, assigning a threshold for the GSS which varies according to the algorithm used, the software categorizes the tumours as either proficient or deficient for homologous recombination. However, the biological reality of HRD in different tumour types might deviate from these parameters, and these platforms offer the opportunity to go deeper in the causes of HRD and genomic instability and identify biomarkers which could be involved in the phenotype beyond *BRCA1/2* and other HRR genes.

While genomic scars can be considered the endpoint of HRD, functional assays, i.e., the formation of RAD51 foci, alone or in combination with HRD scores can provide further sensitivity and specificity in identifying patients likely to benefit from PARPi[29–31]. Response to cisplatin chemotherapy has also been associated with sensitivity to PARPi. In fact, clinical data support the use of PARPi as maintenance therapy in previously cisplatin-sensitive ovarian cancer patients[32].

Regarding NSCLC, GSS is emerging as a potentially more representative marker for HR status in NSCLC, and the current estimation for the prevalence of HRD in NSCLC ranges from 15 to 20%, depending on the cohort examined and the technique employed to assess HR status[33]. Specifically for NSCLC patients with adenocarcinoma, the GSS, particularly when combined with complete TP53 loss, is associated with extremely poor prognosis[14]. On the other hand, it appears that h-GSS tumours could respond better to platinum-based therapy[34] and our observations also support this notion. Preclinical experiments in human cell lines of NSCLC have shown very promising results[35]. To this date, however, the literature is quite poor with regards to functional studies which would allow the identification of NSCLC patients who could really benefit from PARPi. Such information would allow the better design of clinical trials which would really address the clinical potential of PARPi in this devastating disease.

In the current work, we employed GSS assessment as a method to evaluate the HR status of early-stage, operable NSCLC and examine whether PARPi can be beneficial for patients with high scarring scores. Using commercially available diagnostic assays and platforms, we identified a substantial portion of these tumours that present a high genomic scarring score, indicating HRD. Analysis of the mutation profile of HRR-related genes showed that HRD h-GSS tumours do not necessarily carry pathogenic mutations in any of the HRR genes. Conversely, not all tumours carrying pathogenic HRR mutations present a high GSS, information which becomes particularly relevant if patients are to be screened for PARPi administration based solely on HRR gene mutations. Interestingly, a high GSS score is significantly associated with pathogenic TP53 mutations, although the precise molecular mechanisms explaining this association are still under investigation. In agreement with our findings, previous reports have identified the combined presence of TP53 and other mutations as a strong indicator of HRD[8]. Importantly, we show that the variant allele frequency of TP53 mutations significantly aligns with GSS, indicating a possible causal relationship. In agreement with a recent report[14], patients with high GSS and mutations in TP53 show an extended DFI and OS following cisplatin-based chemotherapy. Functionally, HRD was corroborated in PDXs with RAD51 foci measurements in steady-state and cisplatin-treated PDXs, which showed that tumours with high GSS failed to efficiently assemble the HRR machinery. Importantly, treatment with olaparib significantly delayed tumour growth in h-GSS but not in l-GSS PDXs despite the fact that 4/5 h-GSS PDX developed harboured no HRR mutations.

Taken together, our data indicate that the GSS could better serve as a biomarker for HR status in early-stage NSCLC compared to the mere screening of germline or somatic HRR gene mutations and that a combinatorial approach would be the more informative one for clinical practice. Patient stratification based on the GSS could help identify sub-cohorts of patients that would benefit from PARPi administration. Given the strong indications of improved clinical outcomes for platinum-based therapy and immunotherapy in HRD NSCLC, the exciting prospect of combination therapy with PARPi for this subgroup warrants further investigation both in the preclinical and clinical setting.

Methods

Patients

Patients with histologically documented NSCLC, aged >18 years old and clinical stage IA-IIIA, amenable to surgical resection, were enroled in a multicenter, single-arm, translational research study, conducted by the Hellenic Oncology Research Group (HORG), which evaluated the molecular heterogeneity of the disease. This study was performed according to the ethical standards of the 1975 Declaration of Helsinki, as revised in 2008, and was approved by the Ethics and Scientific Committees of the participating hospitals [Metropolitan General Hospital (308/28-12-2017) and 'Sotiria' General Hospital (1288/17-01-2018), Athens, Greece]. All patients gave their written informed consent for both the identification of germline HRR gene mutations and for the somatic mutational profiling of the tumour as well as for the use of their biologic material for research purposes.

A total of 136 patients were enroled during the study period (Table 3). Their median age was 68.0 years old (range, 39–86) and 98 (72.1%) were men. Sixty-seven (49.3%) patients were current smokers and 39 (28.7%) were ex-smokers. Histology was Squamous Cell Carcinoma (SCC) in 56 (41.2%) patients and adenocarcinomas (ADC) in 71 (52.2%); other histological types were rare such as mixed SCC/ADC ($n = 2$ pts) and LCNEC ($n = 7$ pts) (Table 3). Seventy (51.5%) patients had pathological stage I (A and B) disease, whereas 28 (20.6%) and 37 (27.2%) had stage II (A and B) and IIIA disease, respectively (Table 3).

HRD assessment by genomic scarring score calculation via NGS

Genomic DNA from all patients was used to assess the HRD by calculating a GSS facilitated by NGS data analysis. Briefly, DNA was extracted from fresh frozen biopsies (QIAamp DNA Mini kit, QIAGEN), followed by library preparation according to the manufacturer's protocol (AmoyDx® HRD Focus Panel, Amoy Diagnostics Co., Ltd,

China). The constructed libraries were sequenced on a NextSeq550 NGS sequencer (Illumina, San Diego, US). Bioinformatic analysis was performed using the AmoyDx NGS Data Analysis System (ANDAS) which incorporates proprietary algorithms to determine genomic instability by calculating a genomic scaring (GS) score for each sample, based on data from ≈24,000 genome-wide distributed SNPs. The AmoyDx GS model is built on machine learning and it measures genomic instability by weighing different types of chromosomal copy

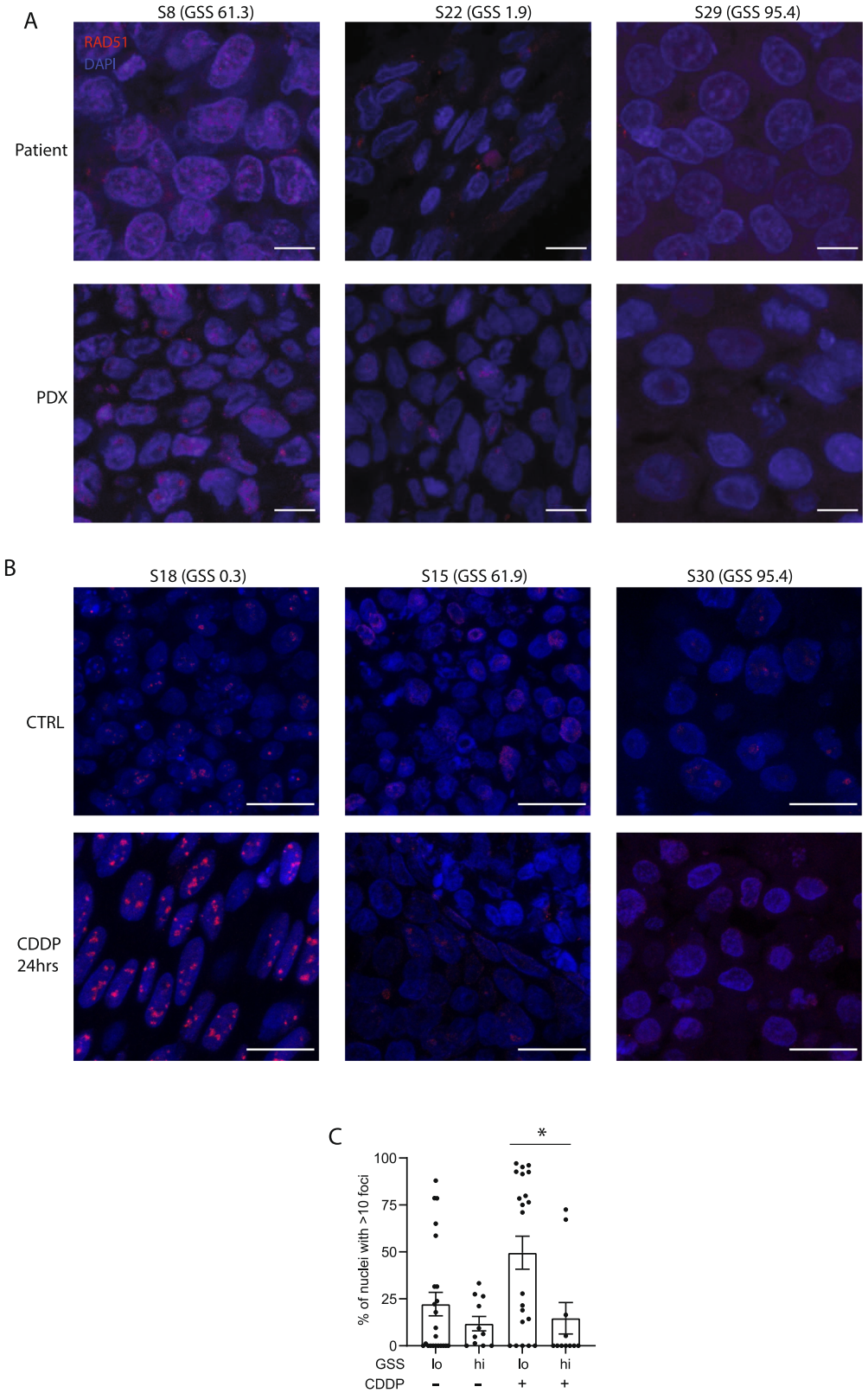

Fig. 4 | Frequency of RAD51 foci upon CDDP treatment. A Comparison of RAD51 foci formation in primary tumours and PDX, representative of 6 different comparisons, scale bar 10 µm. **B** Response of h-GSS and l-GSS PDXs to in vivo DNA damage induction (6 mg/kg CDDP for 24 h), scale bars 20 µm. **C** Quantification of (**B**), percentage of nuclei with >10 RAD51 foci in l-GSS ($n = 7$) vs h-GSS ($n = 4$) PDX, *: $p < 0.05$, 3 different fields per sample were quantified.

numbers[36]. Chromosomal copy number is grouped according to the combination of length of copy number (LCN), type of copy number (TCN), and site of copy number (SCN), while the pipeline has been trained using ovarian cancer datasets. A GSS ranging from 0 to 49 (<50) and from 50 to 100 (>50) was considered as a negative or low GSS (l-GSS) and positive or high (h-GSS) result respectively according to the manufacturer.

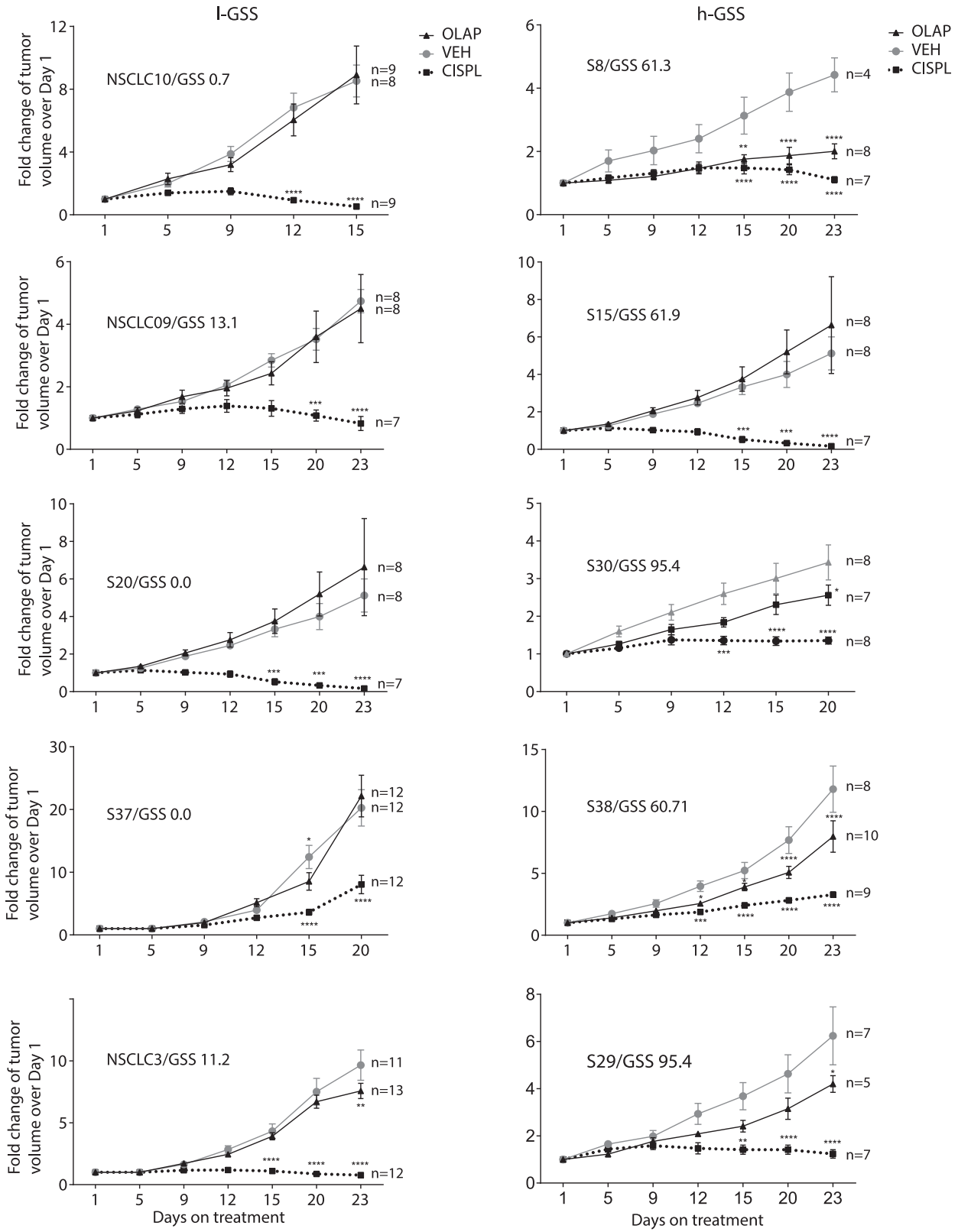

Fig. 5 | Response of l-GSS vs h-GSS PDX to olaparib administration. Statistical significance was determined with 2-way ANOVA and significance per time point was determined via multiple comparisons analysis, *: $p < 0.05$, **: $p < 0.01$, ***: $p < 0.001$, ****: $p < 0.0001$. Patient number, GSS and cohort sizes are indicated for each experiment.

Table 3 | Demographic and other characteristics of the patient cohort

N = 136	No (%)
Age	
Median (min-max)	68.0 (39–86)
Sex	
Men	98 (72.1)
Women	38 (27.9)
Smoking status	
Current	68 (50.0)
Ex-smoker	38 (27.9)
Never	4 (2.9)
N/A	26 (19.1)
Histology	
SCC	55 (40.4)
ADC	71 (52.2)
Mixed	2 (1.5)
LCNEC	8 (5.9)
Stage at diagnosis	
IA	33 (24.3)
IB	36 (26.5)
IIA	8 (5.9)
IIB	20 (14.7)
IIIA + IIIB	38 (27.9)
NA	1 (0.7)
Adjuvant Chemo	
Yes	70 (51.5)
No	62 (45.6)
NA	4 (2.9)
Adjuvant RT	
Yes	7 (5.1)
No	119 (87.5)
NA	10 (7.4)
Relapses	
Yes	45 (33.1)
No	91 (66.9)
DFS (median, min-max)	**NE (0.1–68.4)**
Deaths	
Yes	31 (22.8)
No	105 (77.2)
OS (median, min-max) 1-Year OS	**NE (0.1–68.6) 91.3%**
Follow-up (median, min-max)	**47.9 (0.1–68.6)**

Germline and somatic tumoral HRR gene mutational status

DNA extracted from the PBMCs of 121 (89%) of 136 patients was used in order to assess the presence of germline HRR gene mutations using a commercial panel (AmoyDx ® HANDLE HRR NGS Panel). The used panel, which allowed a reversible terminator sequencing, is intended for the qualitative detection of *AR, ATM, ATR, BARD1, BRCA1, BRCA2, BRIP1, CDH1, CDK12, CHEK1, CHEK2, ESR1, FANCA, FANCL, HDAC2, HOXB13, MRE11A, NBN, PALB2, PPP2R2A, PTEN, RAD51B, RAD51C, RAD51D, RAD54L, STK11* and *TP53* gene variants (in complete coding exons and exon-intron boundaries). The detected variants include point mutations, small insertions, and deletions in HRR genes.

DNA extracted from 140 fresh-frozen biopsies was also used to assess somatic mutations and library construction using a commercial panel (AmoyDx® HRD Complete Panel, Amoy Diagnostics Co.) that has all the same characteristics as the AmoyDx® HRD Focus Panel described before, but also includes the mutational analysis (SNV/InDels and homozygous deletions) of 20 homologous recombination repair (HRR) related genes: *ATM, BARD1, BRCA1, BRCA2, BRIP1, CDH1, CDK12, CHEK1, CHEK2, FANCA, FANCL, HDAC2, PALB2, PPP2R2A, PTEN, RAD51B, RAD51C, RAD51D, RAD54L, TP53*. Four (2.9%) samples failed QC metrics and therefore were excluded from the results (Supplementary Table 5).

Mouse colony management

Immunocompromised *NOD.Cg-Prkdcscid Il2rgtm1Wjl/SzJ* (NSG) mice were purchased from Harlan and kept in separate ventilated cages in a controlled environment free from specific pathogens, following the guidelines set by FELASA (Federation of Laboratory Animal Science Associations), at the Animal House Facility of the Biomedical Research Foundation of the Academy of Athens (BRFAA, Greece). All animal care and treatment procedures were reviewed and approved by the Institutional Committee on Ethics of Animal Experiments. The animal handling protocol for this project was licensed under 812701-03/07/2023.

Establishment of patient-derived xenografts (PDX)

For the establishment of PDX, primary tumour material not needed for diagnostic purposes was used. After the resection of biopsies for DNA and RNA extraction, the remaining material was cut into pieces of up to 4mmX4mm. The pieces were implanted in the flanks of NSG mice via small (0.5 cm) incisions using sterile forceps. The incisions were then stapled shut using the Autoclip system (Agntho's AB, Autoclip Clips, Applier 9 mm, 12020-09, Sweden). Implanted tumours were monitored for growth by measuring twice a week using a calliper (Insize, 1205-1502S, China). When tumours reached a diameter of 1 cm, mice were sacrificed, and tumours were cut in pieces of 2mmX2mm for passage and expansion. Cohorts were deemed complete when we had at least $n = 20$ different mice harbouring one PDX per flank from the original tumour.

Drug testing on PDX

Drug administration (vehicle, cisplatin or olaparib) was initiated when tumours reached a size of 4 mm × 4 mm. All drugs were administered intraperitoneally. For CDDP (Pharmachemie BV, 21C28LB, Netherlands), 6 mg/kg was administered once weekly, whereas for Olaparib (MedchemExpress, HY-10162, Sweden) 50 mg/kg was administered daily. Tumours were measured as described twice weekly and mice were sacrificed when tumours reached the humane endpoint, usually not longer than 25 days post-treatment initiation. For damage induction and RAD51 assessment, untreated mice with PDX of at least 7 mm × 7 mm were treated intraperitoneally with 6 mg/kg of cisplatin and sacrificed 24 or 72 h later.

Real-time quantitative PCR (qPCR) for gene expression analysis

Total mRNA was extracted from the patients' snap-frozen biopsies using the E.Z.N.A. kit (Omega, E1091 -02, USA) according to the provider's instructions. On-column genomic DNA digestion was performed. Reverse transcription (RT) was carried out from 1 μg of total mRNA using the RT Reagent Kit PrimeScript (Takara, RR037A, Japan) according to the provider's instructions. qPCR was performed in duplicate for every gene including three different housekeeping genes using 25 ng of total mRNA per reaction. Fluorescence was detected using SYBRgreen dye (Biorad, 172 -5124, USA). A detailed list of all primer pairs used can be found in Supplementary Table 6.

Tissue processing and staining for confocal microscopy

Sections from patients' paraffin blocks were obtained from the Histopathology Department of the Sotiria General Hospital. PDX tumours were excised from the mice at the endpoint of the experiments. Small biopsies

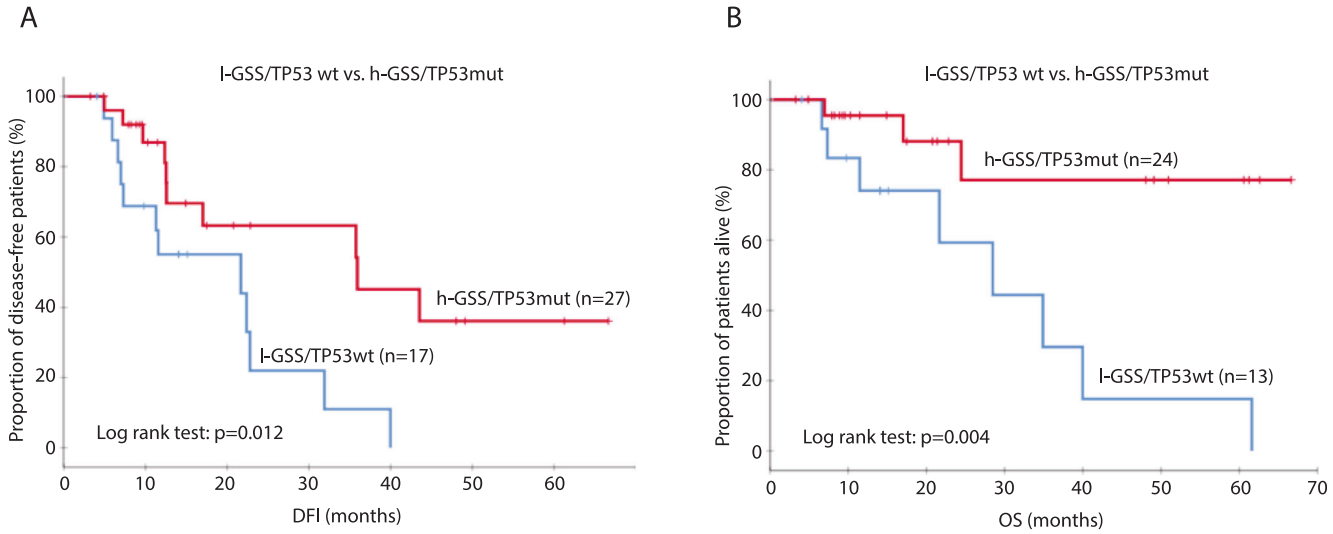

Fig. 6 | Predictive value of GSS and TP53 status in platinum response. A DFI of patients treated with platinum-based chemotherapy in the adjuvant setting. **B** OS of patients treated with platinum-based chemotherapy at any line.

were snap-frozen for DNA and RNA extraction, and the remaining tissue was fixed in 4% PFA overnight (ON) at room temperature (RT). The following day, tissues were transferred in 70% ethanol and processed for paraffin embedding in a Leica Tissue processor. 5 µm-thick sections were cut in a semi-automatic Leica RM2125 microtome (Leica Instruments, Singapore) and placed on slides pre-treated with poly-L-lysine (Menzel-Thermo, 19352000, USA). Deparaffinization and staining were performed as previously described. Briefly, citrate buffer was used for antigen retrieval (1 h, 120 °C) and non-specific binding was blocked by incubating the slides in blocking solution (PBS/BSA 0.5%/Triton 0.5%) for 1 h at RT. Primary antibody against RAD51 (Abcam, ab133534, UK) was then placed on each slice and incubated ON at 4 °C. Slices were washed three times in PBS/Triton 0.5% and a secondary anti-Rabbit-Cy5 antibody (Jackson ImmunoResearch, AB_2338013, USA) in PBS was incubated for 1 h at RT. After 3 washes in PBS, slices were stained with DAPI (Vector, H-1200, USA) for 3 min at RT, washed, and mounted with Mowiol mounting medium. Staining was visualized the following day and up to 10 days later under a Leica Inverted SP5 confocal microscope.

RAD51 foci quantification

To evaluate the recruitment of the HRR machinery to damage sites, the formation of RAD51 foci was assessed before and after damage induction on PDX with cisplatin. We quantified 3 different controls and 3 different cisplatin-treated fields from $n = 7$ Homologous Recombination proficient (HRP) and $n = 4$ HRD PDX. We considered responsive nuclei with over 10 RAD51 foci and normalized this count with the total number of nuclei per field.

Statistical analysis

For the clinical data and mutational analysis summary tables (descriptive statistics and/or frequency tables) were provided for all baseline and efficacy variables, as appropriate. Continued variables were summarized with descriptive statistics (n, median and range). Qualitative factors were compared by Pearson's chi-square test or Fisher's exact test, when appropriate. Disease-free interval (DFI) was defined as the time from the date of NSCLC initial diagnosis to the date of the first documented relapse/recurrence or death from any cause, whichever occurred first. Overall survival (OS) was defined as the time from the date of NSCLC initial diagnosis to the date of death from any cause. Patients alive without any predefined event (recurrence/relapse or death) were considered as censored at the time of the last known follow-up assessment. Time-to-endpoint events (DFI, OS) were estimated using the Kaplan–Meier method and the comparisons were computed with the log-rank test. Median follow-up was calculated using the reverse Kaplan-Meier method. All statistical tests were two-sided, and p-values < 0.05 were considered statistically significant. The data were analyzed using IBM SPSS statistics (Version 26.0) predictive analytic software. Statistical analysis of the experimental data was carried out using GraphPad Prism and SPSS software.

Data availability

The datasets produced and analysed during the current study are available from the corresponding author upon reasonable request.

Received: 10 July 2024; Accepted: 6 December 2024;
Published online: 26 December 2024

References

1. Moynahan, M. E. & Jasin, M. Mitotic homologous recombination maintains genomic stability and suppresses tumorigenesis. *Nat. Rev. Mol. Cell Biol.* **11**, 196–207 (2010).
2. Bryant, H. E. et al. Specific killing of BRCA2-deficient tumours with inhibitors of poly(ADP-ribose) polymerase. *Nature* **434**, 913–917 (2005).
3. Farmer, H. et al. Targeting the DNA repair defect in BRCA mutant cells as a therapeutic strategy. *Nature* **434**, 917–921 (2005).
4. Coleman, R. L. et al. Rucaparib maintenance treatment for recurrent ovarian carcinoma after response to platinum therapy (ARIEL3): a randomised, double-blind, placebo-controlled, phase 3 trial. *Lancet* **390**, 1949–1961 (2017).
5. Robson, M. et al. Olaparib for Metastatic Breast Cancer in Patients with a Germline BRCA Mutation. *N. Engl. J. Med* **377**, 523–533 (2017).
6. Pujade-Lauraine, E. et al. Olaparib tablets as maintenance therapy in patients with platinum-sensitive, relapsed ovarian cancer and a BRCA1/2 mutation (SOLO2/ENGOT-Ov21): a double-blind, randomised, placebo-controlled, phase 3 trial. *Lancet Oncol.* **18**, 1274–1284 (2017).
7. Litton, J. K. et al. Talazoparib in patients with advanced breast cancer and a germline BRCA mutation. *N. Engl. J. Med.* **379**, 753–763 (2018).
8. Riaz, N. et al. Pan-cancer analysis of bi-allelic alterations in homologous recombination DNA repair genes. *Nat. Commun.* **8**, 857 (2017).
9. Gachechiladze, M., Skarda, J., Soltermann, A. & Joerger, M. RAD51 as a potential surrogate marker for DNA repair capacity in solid malignancies. *Int J. Cancer* **141**, 1286–1294 (2017).

10. Telli, M. L. et al. Homologous Recombination Deficiency (HRD) score predicts response to platinum-containing neoadjuvant chemotherapy in patients with triple-negative breast cancer. *Clin. Cancer Res.* **22**, 3764–3773 (2016).
11. Rempel, E. et al. Pan-cancer analysis of genomic scar patterns caused by homologous repair deficiency (HRD). *NPJ Precis Oncol.* **6**, 36 (2022).
12. Shim, J. H. et al. HLA-corrected tumor mutation burden and homologous recombination deficiency for the prediction of response to PD-(L)1 blockade in advanced non-small-cell lung cancer patients. *Ann. Oncol.* **31**, 902–911 (2020).
13. Kadouri, L. et al. Homologous recombination in lung cancer, germline and somatic mutations, clinical and phenotype characterization. *Lung Cancer* **137**, 48–51 (2019).
14. Feng, J. et al. Combination of genomic instability score and TP53 status for prognosis prediction in lung adenocarcinoma. *NPJ Precis Oncol.* **7**, 110 (2023).
15. Fennell, D. A. et al. Olaparib maintenance versus placebo monotherapy in patients with advanced non-small cell lung cancer (PIN): A multicentre, randomised, controlled, phase 2 trial. *EClinicalMedicine* **52**, 101595 (2022).
16. Takamatsu, S. et al. Utility of homologous recombination deficiency biomarkers across cancer types. *JCO Precis Oncol.* **6**, e2200085 (2022).
17. Kanaki, Z. et al. Generation of non-small cell lung cancer patient-derived xenografts to study intratumor heterogeneity. *Cancers.* **13**, https://doi.org/10.3390/cancers13102446 (2021).
18. Wang, D. et al. Molecular heterogeneity of non-small cell lung carcinoma patient-derived xenografts closely reflect their primary tumors. *Int J. Cancer* **140**, 662–673 (2017).
19. Chen, Y. et al. Tumor characteristics associated with engraftment of patient-derived non-small cell lung cancer xenografts in immunocompromised mice. *Cancer* **125**, 3738–3748 (2019).
20. Klinakis, A., Karagiannis, D. & Rampias, T. Targeting DNA repair in cancer: current state and novel approaches. *Cell Mol. Life Sci.* **77**, 677–703 (2020).
21. Lord, C. J. & Ashworth, A. PARP inhibitors: synthetic lethality in the clinic. *Science* **355**, 1152–1158 (2017).
22. McCabe, N. et al. Deficiency in the repair of DNA damage by homologous recombination and sensitivity to poly(ADP-ribose) polymerase inhibition. *Cancer Res.* **66**, 8109–8115 (2006).
23. da Cunha Colombo Bonadio, R. R., Fogace, R. N., Miranda, V. C. & Diz, M. Homologous recombination deficiency in ovarian cancer: a review of its epidemiology and management. *Clinics* **73**, e450s (2018).
24. Batalini, F. et al. Comparison of PARPi efficacy according to homologous recombination deficiency biomarkers in patients with ovarian cancer: a systematic review and meta-analysis. *Chin. Clin. Oncol.* **12**, 21 (2023).
25. Watkins, J. A., Irshad, S., Grigoriadis, A. & Tutt, A. N. Genomic scars as biomarkers of homologous recombination deficiency and drug response in breast and ovarian cancers. *Breast Cancer Res.* **16**, 211 (2014).
26. Marquard, A. M. et al. Pan-cancer analysis of genomic scar signatures associated with homologous recombination deficiency suggests novel indications for existing cancer drugs. *Biomark. Res.* **3**, 9 (2015).
27. Mark, L. R. et al. Homologous recombination deficiency detection algorithms: a systematic review. *Cancers.* **15**, https://doi.org/10.3390/cancers15235633 (2023).
28. Brown, L. C. et al. RNA-based homologous recombination deficiency signature detects homologous recombination deficiency-RNA+ patients with and without homologous recombination repair gene pathogenic alterations in men with prostate cancer. *JCO Precis Oncol.* **7**, e2300378 (2023).
29. Korsholm, L. M. et al. Combining homologous recombination-deficient testing and functional RAD51 Analysis enhances the prediction of Poly(ADP-Ribose) polymerase inhibitor sensitivity. *JCO Precis Oncol.* **8**, e2300483 (2024).
30. van Wijk, L. M., Nilas, A. B., Vrieling, H. & Vreeswijk, M. P. G. RAD51 as a functional biomarker for homologous recombination deficiency in cancer: a promising addition to the HRD toolbox? *Expert Rev. Mol. Diagn.* **22**, 185–199 (2022).
31. Llop-Guevara, A. et al. Association of RAD51 with homologous recombination deficiency (HRD) and clinical outcomes in untreated triple-negative breast cancer (TNBC): analysis of the GeparSixto randomized clinical trial. *Ann. Oncol.* **32**, 1590–1596 (2021).
32. O'Malley, D. M., Krivak, T. C., Kabil, N., Munley, J. & Moore, K. N. PARP inhibitors in ovarian cancer: a review. *Target Oncol.* **18**, 471–503 (2023).
33. Mekonnen, N., Yang, H. & Shin, Y. K. Homologous recombination deficiency in ovarian, breast, colorectal, pancreatic, non-small cell lung and prostate cancers, and the mechanisms of resistance to PARP inhibitors. *Front. Oncol.* **12**, 880643 (2022).
34. Zhang, L., Guan, S., Meng, F., Teng, L. & Zhong, D. Next-generation sequencing of homologous recombination genes could predict efficacy of platinum-based chemotherapy in non-small cell lung cancer. *Front. Oncol.* **12**, 1035808 (2022).
35. Ji, W. et al. Non-small cell lung cancer cells with deficiencies in homologous recombination genes are sensitive to PARP inhibitors. *Biochem. Biophys. Res. Commun.* **522**, 121–126 (2020).
36. Yuan, W. et al. Genomic Scar Score: a robust model predicting homologous recombination deficiency based on genomic instability. *BJOG* **129**, 14–22 (2022).

Acknowledgements

We thank the patients and their families for participating in this study. We thank the Imaging Unit, the Histology Core facility and the Greek Genome Center of the Biomedical Research Foundation of the Academy of Athens. We would like to thank Amoy Diagnostics for providing the HRR panels and covering sequencing expenses. This work was supported in part by the EU grants Tumour-LN-oC (Grant agreement ID: 953234) and MULTIR (Grant agreement ID: 101136926).

Author contributions

Conceptualization: A.K. and V.G. Experiment design: A.K., K.T. and V.G. Experiment implementation: K.T., A.C., G.C., A.V., K.P., I.V., D.H., G.Z., and G.V. Result investigation: K.T., P.C., G.C., A.V., V.G., At.K. and A.K. Funding acquisition: A.K. and V.G. Project administration: A.K. and V.G. Supervision: P.C., V.G. and A.K. Writing—original draft: K.T and A.K. Writing—review & editing: K.T., P.C., A.V., D.H., V.G. and A.K.

Competing interests

The authors declare no competing interests.

Additional information

Supplementary information The online version contains supplementary material available at https://doi.org/10.1038/s41698-024-00777-6.

Correspondence and requests for materials should be addressed to Apostolos Klinakis.